

Recent X-Ray Observations of SN1986J with ASCA and ROSAT

John C. Houck¹, Joel N. Bregman²

University of Michigan, Department of Astronomy, Dennison Bldg., Ann Arbor, MI, 48109-1090

Roger A. Chevalier³

University of Virginia, Department of Astronomy, P.O. Box 3818, University Station,
Charlottesville, VA 22903-0818

Kohji Tomisaka⁴

Laboratory of Physics, Faculty of Education, Niigata University, Ikarashi 2-8050, Niigata 950-21,
Japan

ABSTRACT

We have presented *ASCA* and *ROSAT* observations of SN 1986J covering the period 1991 August to 1996 January. From observations with the *ROSAT HRI* and *PSPC*, we find that the 0.5-2.5 keV flux decreased $\propto t^{-2}$ during this period; the *ASCA* data are consistent with this result and extend it to the 2-10 keV band. *ASCA* spectra from 1994 January and 1996 January are consistent with thermal emission from a solar metallicity plasma at an equilibrium temperature $kT = 5-7.5$ keV, somewhat hotter than that observed from other X-ray supernovae. These spectra also show a clear Fe K emission line at 6.7 keV with $\text{FWHM} < 20,000 \text{ km s}^{-1}$ (90% confidence). This limit on the line width is consistent with the reverse shock model of Chevalier & Fransson (1994), but does not rule out the clumpy wind model of Chugai (1993).

Subject headings: supernovae: individual (SN 1986J) — X-rays: general

1. Introduction

A few supernovae have been detected as sources of soft X-ray emission in the first decades after the supernova event (Canizares Kriss & Feigelson 1982; Tanaka 1989; Gorenstein, Hughes & Tucker 1994; Bregman & Pildis 1992; Ryder *et al.* 1993; Zimmerman, *et al.* 1993; Tanaka 1993;

¹MIT, Center for Space Research, 70 Vassar St., Bldg. 37-662B, Cambridge, MA 02139-4307, houck@space.mit.edu

²jbregman@astro.lsa.umich.edu

³rac5x@virginia.edu

⁴tomisaka@pulsar.mtk.nao.ac.jp

Fabian & Terlevich 1996). All of the detected sources are associated with Type II supernovae and, judging from radio observations, the most X-ray luminous of these appear to have had extensive circumstellar winds (Schlegel 1995 and references therein). The interaction between the shock wave generated by the supernova with a dense circumstellar environment is expected to produce both soft X-ray emission and synchrotron radio emission (Chevalier 1982; Chevalier & Fransson 1994, hereafter CF). There are two competing models for the production of this soft X-ray emission; here we present observations that help to discriminate between the two models and define the constraints for further model development.

Type II supernovae are associated with massive stars that, during their supergiant phase, drove slow, dense winds prior to the supernova event. If the wind material is smoothly distributed, the exploded star will drive a fast high temperature shock (the blast shock) into the wind, with velocities of 10,000-20,000 km s⁻¹ and temperatures of 10⁹ K. Also, a relatively slow shock (the reverse shock) propagates back into the stellar envelope at a velocity of 500-1000 km s⁻¹ relative to the expanding ejecta. This relatively mild shock-deceleration of the stellar envelope produces 10⁷ K gas that can account for the soft X-ray emission detected with X-ray telescopes. Little X-ray radiation emerges from the dilute 10⁹ K gas behind the blast shock, although particle acceleration in the shocked shell can produce non-thermal radio emission (Chevalier 1982; CF).

The situation can be substantially different if either the circumstellar wind material or the exploded stellar envelope is highly clumped. The case of a highly clumped circumstellar wind has been studied by Chugai (1993) and applied to SN 1986J. His study was motivated by the observation of narrow Balmer emission lines (< 600 km s⁻¹; Leibundgut et al. 1991) in the optical spectrum of SN 1986J. This observation was surprising since hydrogen emission lines are usually identified with the outer part of the exploded star, which for SN 1986J, is expanding at ~10,000 km s⁻¹ (based upon its age and radio VLBI size; Bartel, Rupen, and Weiler 1989). Chugai (1993) proposed that the progenitor wind was clumpy and that the narrow emission lines and the soft X-ray emission originate in the wind clumps or clouds. In this model, the reverse shock is too weak to produce observable soft X-rays. Rather, it is the pressure in the strongly shocked wind that crushes the embedded clouds, driving shocks into the clouds. The observed soft X-rays are produced by radiative cooling of shocked cloud material, and the Balmer emission is produced when these soft X-rays are reprocessed in the cooler cloud material. The inertia of the clouds is so great that they are not accelerated outward when the blast shock passes over them, so the FWHM of the optical emission lines reflects only the speed of the shock driven into the clouds. Because the reverse shock model predicts X-ray lines of order 10,000 km s⁻¹ wide, the line widths of the X-ray emission lines, which can be observed with *ASCA*, can be a powerful discriminator between the reverse shock model and model of Chugai (1993).

X-ray emission in young supernovae has been observed in only a few cases (SN 1978K, 1980K, 1986J, 1987A, 1988Z, 1993J, and 1995N), and of these, only two are bright enough to obtain both spectra and fluxes: SN 1986J and 1993J. SN 1986J, in the nearby edge-on spiral galaxy NGC 891, was first discovered in the radio (Rupen et al. 1987) and is one of the closest recent supernovae.

Because of its large radio luminosity, SN1986J is thought to have had a progenitor red supergiant star with an unusually dense wind (Weiler, Panagia, and Sramek 1990) and was predicted to be luminous in soft X-rays (Chevalier 1987). An August 1991 *PSPC* observation (Bregman and Pildis 1992) confirmed that it is X-ray luminous. Based on this *PSPC* observation, the X-ray emission was characterized by $L_x(0.1 - 2.5 \text{ keV}) = (1.6 - 7) \times 10^{40} \text{ erg s}^{-1}$, $T_x = 1.0 - 3.9 \text{ keV}$, and an absorbing column of $(5 - 14) \times 10^{21} \text{ cm}^{-2}$. Because of the high absorption column, most of the photons were removed from the low energy band of the *ROSAT PSPC* so that the received X-ray photons fell into a very limited energy range (0.7-2 keV), and the temperature and luminosity were poorly determined. Nevertheless, these *PSPC* measurements, when combined with radio data, gave a consistent fit to the reverse shock model (CF).

Four new observations were obtained during the past five years: a second *ROSAT PSPC* observation, a *ROSAT HRI* observation, and two *ASCA* observations. The *ROSAT* and *ASCA* observations provide clear evidence of dimming while the *ASCA* observations determine the abundance, temperature, and line width of the X-ray emitting material. Here, we present these recent observations and compare these new results with the theoretical expectations for the competing models.

2. Observations and Analysis

2.1. *ROSAT* Observations of SN 1986J

2.1.1. *PSPC* Observations

The first observation of SN 1986J, obtained on August 18, 1991 (as part of AO1), consists of 24.9 ksec of live time data, which included some periods where the background was more than twice the modal background level; nearly all of the higher background levels are identified with scattered solar X-rays. We discarded observing periods when the background exceeded 1.7 times the modal background value, which yielded a remaining live time of 17.1 ksec. In the initial analysis of these data (Bregman and Pildis 1992), no data were discarded, but the difference in spectral fits and fluxes between the two types of analysis are insignificant. The second observation of SN 1986J was obtained 23 months later, during the period July 8-27, 1993 (as part of AO4), and consists of 31.5 ksec of useful observing time. There are no periods during which the background became high relative to the modal value of the background, so no data were excluded. The background, as well as being better behaved than the 1991 observations, has a lower mean value, so low intensity features, such as those associated with the diffuse galactic emission, are seen at a higher signal-to-noise level (Bregman & Houck 1996).

At the resolution of the *PSPC*, the emission from SN 1986J is contaminated by a weaker nearby source and by the diffuse galactic emission. This weaker source is visible in the *PSPC* image in that it causes a distortion in the shape of the emission from SN 1986J (Fig. 1a, 1b),

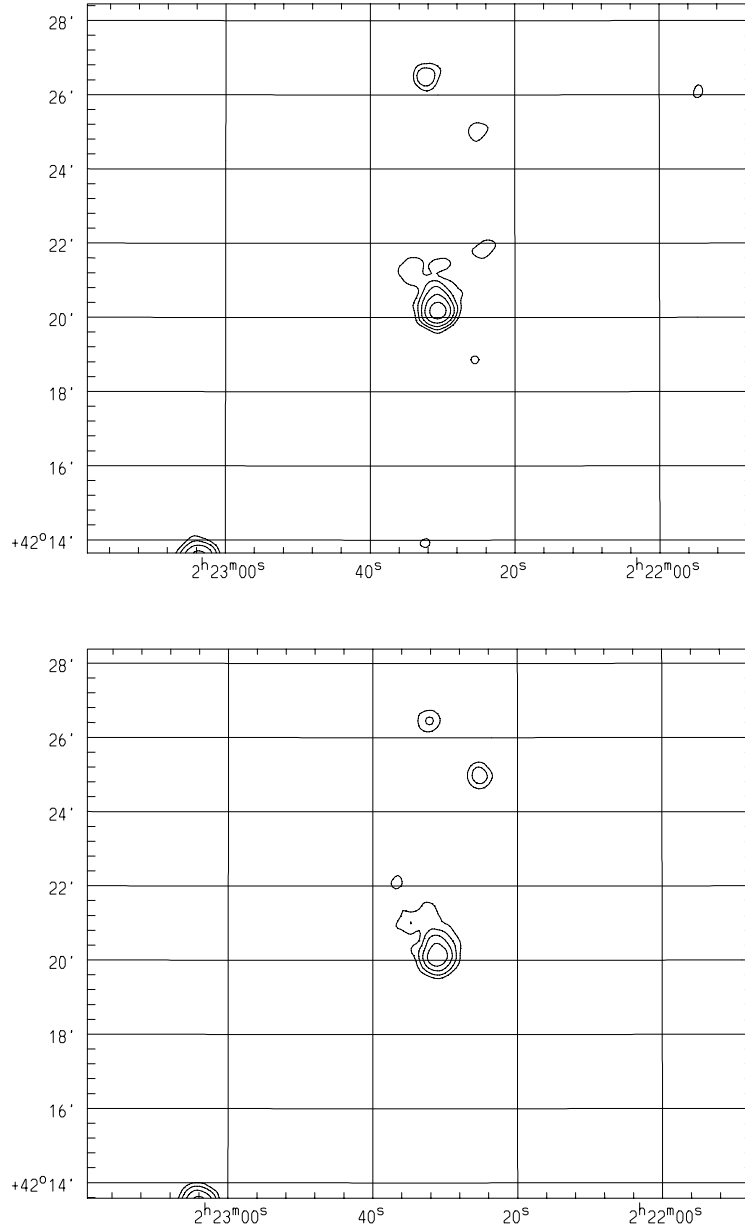


Fig. 1.— *PSPC* images of SN1986J from a) 1991 Aug and b) 1993 Jul. In (a) the contours represent 0.3, 0.6, 1.2, 2.4, and 4.8 counts per 4'' square pixel. In (b) the contour levels have been scaled to the same effective exposure time as in (a), which means that the contour levels are 0.55, 1.11, 2.22, 4.43, and 8.86 counts per 4'' square pixel. The supernova image is elongated because of the weaker source “Xnorth” 27.7'' north and 0.4'' east of the supernova position. The sources are unresolved in the *PSPC*, but are clearly resolved by the *HRI*. Note that most of the extra emission in the field of view is not noise, but is diffuse emission from NGC 891.

but in the *HRI* image (Fig. 2), the two sources are clearly separated, with the weaker source $27.7''$ to the north and $0.4''$ to the east (this source will be referred to as Xnorth in the tables). In the extraction of *PSPC* fluxes for SN 1986J, we fit point sources to the data, where the point spread function (PSF) is approximated by a Gaussian profile and the relative source separation is given by the *HRI* positions. The amplitude of the two Gaussians was varied until the remaining residuals were similar to those expected from photon noise and where the emission from the underlying galaxy was approximately continuous (the galaxy contribution is small). The resulting count rates for SN 1986J and source Xnorth are listed in Table 1.

For spectral analysis we used a $25''$ diameter aperture centered on the supernova minus the background in an annulus of interior and exterior radii $75''$ and $200''$. This background includes the diffuse emission from the galaxy, which should improve the accuracy of the resultant spectra, although the number of background photons is not large in the $25''$ diameter aperture. The $25''$ aperture used encircles 91% of photons from the supernova (at 1 keV), and the use of larger apertures lowered the S/N of the spectrum (the background was increased) without changing the results of the spectral analysis. A single-temperature thermal plasma model (a “Raymond-Smith” plasma) provides a successful fit to the data. Based solely on the *PSPC* data, there are two regions of temperature- N_H space that produce equally acceptable spectral fits, a low temperature (0.2-1 keV) high N_H region ($\log N_H = 22.0-22.5$) and a higher temperature (1-10 keV) lower N_H region ($\log N_H = 21.5-21.9$). This degeneracy is broken by the *ASCA* data, which reveal that the lower column, higher temperature solution is the correct one, and this is the one that will be discussed. The pulse-height spectra from the two periods are quite similar and there was no statistically significant change in the acceptable spectral fits. However, there is an indication that N_H has decreased between 1991 and 1993, as seen in the χ^2 grids (Fig. 3a and Fig. 3b). For the sake of comparison, we adopted two spectral models that give good fits to the two spectra in order to make comparisons of flux and luminosity. The two fits have cosmic abundance and $\log N_H = 21.7$, $T = 2.0$ keV, which is within the 1% contour for each model (Table 1), and $\log N_H = 21.65$, $T = 5.0$ keV, which is about at the 95% confidence contour, and represents a higher temperature case. However, the difference in the absorption corrected flux and the luminosity (columns 6 and 7 in Table 1) were insignificant so only the results of the 2 keV model are shown in Table 1.

2.1.2. The *HRI* Observation

The *HRI* observations were obtained during 26 Jan 1995 to 4 Feb 1995 for a total useful exposure time of 97.17 ksec. The background was well-behaved during the observation and the image clearly shows the supernova and the source to the north (Fig. 2). Other lower-level emission due to the galaxy can be extracted from the data and are discussed in Bregman & Houck (1996). The count rate was determined within a circle of $13''$ radius, which encircles 90% of the photons from a point source; a 10% correction was applied to compensate for the scattered photons. For the determination of the flux and luminosity, we adopted the same spectrum used for *PSPC*

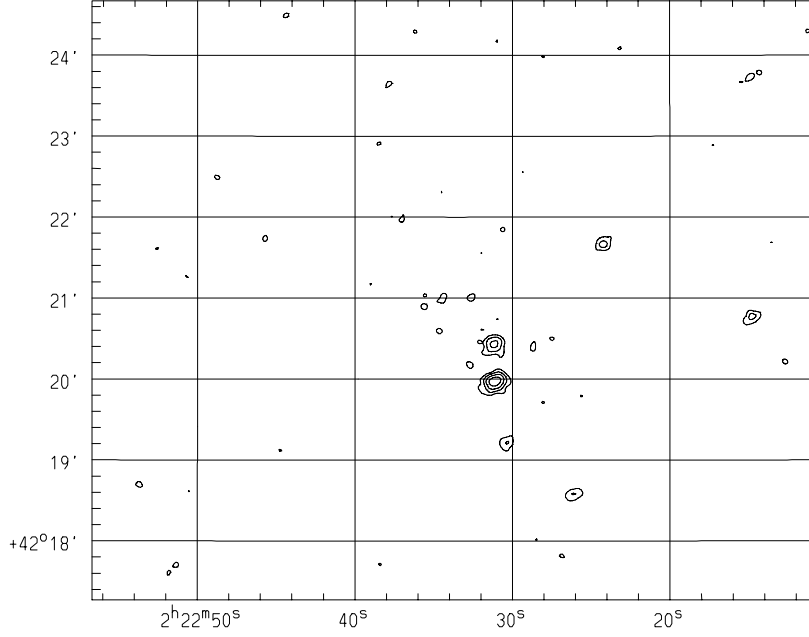


Fig. 2.— 1995 Jan *HRI* image of SN1986J. The nearby weaker point source “Xnorth” is clearly resolved. The contour levels represent 0.35, 0.70, 1.4, and 2.8 counts per $1''$ square pixel. Note that most of the extra emission in the field of view is not noise, but is diffuse emission from NGC 891.

Table 1. *ROSAT* Observations

Obs.	MJD	Instr.	Source	Count Rate (10^{-2} counts s^{-1})	Flux ^a (erg s^{-1} cm^{-2})	L ^a (erg s^{-1})
Aug 1991	48486.1	PSPC	SN1986J	2.38 ± 0.12	7.90(-13)	9.47(39)
			XNorth	0.39 ± 0.05		
Jul 1993	49206.5	PSPC	SN1986J	1.44 ± 0.07	4.91(-13)	5.89(39)
			XNorth	0.37 ± 0.04		
Jan 1995	49744.0	HRI	SN1986J	0.43 ± 0.03	3.95(-13)	4.73(39)
			XNorth	0.17 ± 0.02		

^a $\log N_H = 21.7$; $kT = 2$ keV; energy range 0.5-2.5 keV

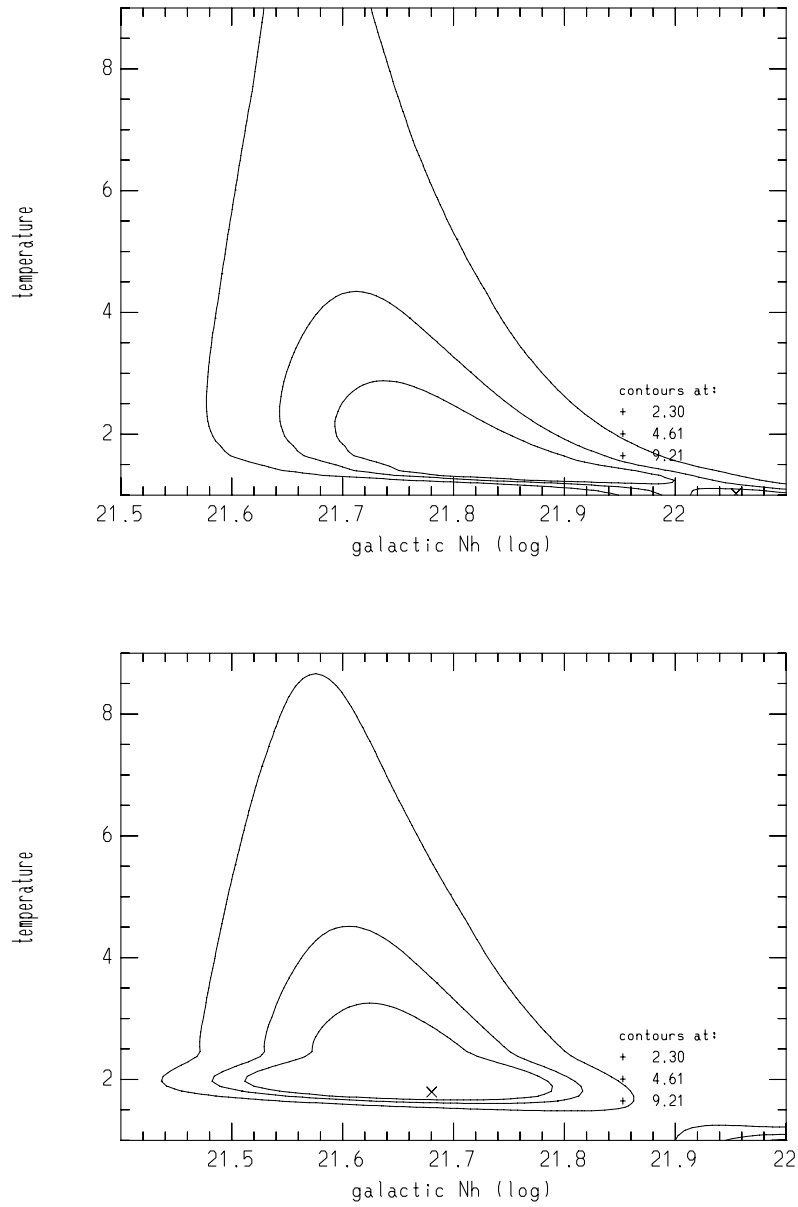


Fig. 3.— Temperature and column density confidence contours for *ROSAT* PSPC spectra from a) 1991 Aug and b) 1993 Jul.

spectral analysis ($\log N_H = 21.7$, $T = 2.0$ keV).

2.2. Time Variability

The clearest difference between the observations is that there has been a significant decrease in the count rate, flux, and luminosity over a three and a half year period. The supernova event probably occurred in the last half of 1982 or the first few months of 1983, so if we assume that the event occurred in 1983.0, then the first *PSPC* observation occurred 8.63 years after the SN event, the second *PSPC* observation occurred 10.61 after the SN and the last *ROSAT* observation was obtained when the remnant was 12.08 years old. The time variation is decreasing approximately as t^{-2} , based upon these three measurements (Fig. 4), although with only three points, the form of the dimming is not well-established.

2.3. ASCA Observations of SN 1986J

SN1986J was observed by *ASCA* during 1994 January 21-22 and again during 1996 January 30-31. Standard criteria were used to exclude data taken during high noise conditions, especially those taken in close proximity to the South Atlantic Anomaly and other regions of low geomagnetic rigidity, and those taken when the line of sight to the supernova lay too close to the limb of the earth. We excluded *GIS* data taken while the ambient magnetic rigidity was less than 6 GeV/c and when the elevation angle above the limb of the earth was less than 5 degrees. For the *SIS* instruments, the cutoff values were 6 GeV/c and 10 degrees (20 degrees for the bright earth), respectively. Charged particle events were excluded from the *SIS* data by retaining only *SIS* events with grade 0,2,3 and 4. X-ray detections were identified and extracted using *GISCLEAN* and *SISCLEAN* within the *XSELECT* reduction package. The net usable exposure times along with the count rates for the extraction regions used (radius R_{extr} arcmin) are given in Table 2. The *GIS* extraction regions were chosen to minimize contamination from a transient X-ray source about 6' NE of the SN position along the galactic disk. Background spectra were obtained from archival blank sky observations using the same extraction regions used for the source spectra. The background subtracted spectra are shown in Figs 5 and 6.

X-ray emission from SN 1986J is superposed on the weak, extended X-ray emission from the host galaxy. *ROSAT PSPC* observations of NGC 891 detect soft X-rays extending to 1'.7 above the plane of the galaxy and 2'.2 radially along the disk of the galaxy (Bregman & Pildis 1994; Bregman & Houck 1996). Because of the broad ($\sim 3'$ half-power radius), asymmetric and energy dependent point spread function (PSF) of the *ASCA* X-ray telescope (XRT), X-ray emission from the supernova is confused with X-ray emission from the galaxy and the nearby point source seen with the *ROSAT HRI*. This makes it difficult to determine the total X-ray flux from the supernova and confuses the interpretation of the X-ray spectrum at low energies, $\lesssim 1$ keV, where emission

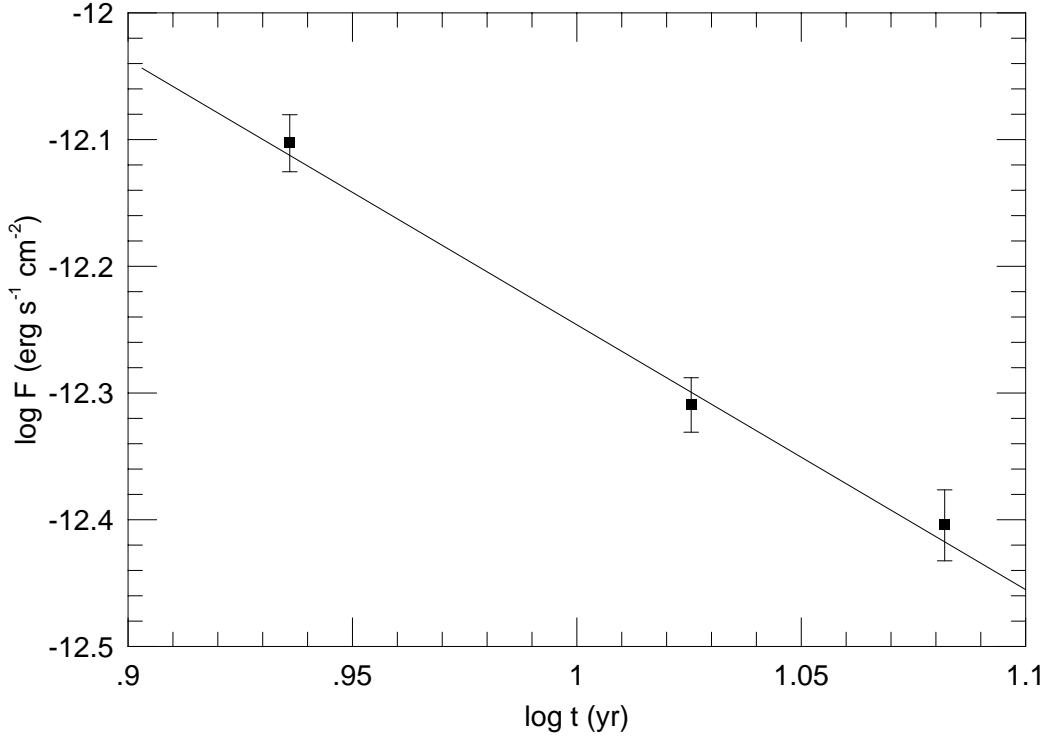


Fig. 4.— X-ray light curve of SN1986J from *ROSAT PSPC* and *HRI* observations. t is the age in years since 1983.0 and F is the unabsorbed flux in $\text{erg s}^{-1} \text{cm}^{-2}$ for an absorbing column of $\log N_H = 21.7$.

Table 2. *ASCA* Observations

Instr.	R_{extr} (arcmin)	MJD 49374.5 (1994 Jan)				MJD 50113.5 (1996 Jan)			
		Exp. (ksec)	$(10^{-2} \text{ counts s}^{-1})$			Exp. (ksec)	$(10^{-2} \text{ counts s}^{-1})$		
			total	bkgd	src		total	bkgd	src
SIS0	2.97	43.8	5.11	1.15	3.96	50.0	4.46	1.19	3.27
SIS1	2.97	41.4	4.48	1.07	3.41	49.8	4.13	1.27	2.86
GIS2	4.70	47.1	4.24	1.34	2.90	54.4	3.59	1.25	2.34
GIS3	4.70	47.2	5.20	1.56	3.64	54.4	4.48	1.48	3.00

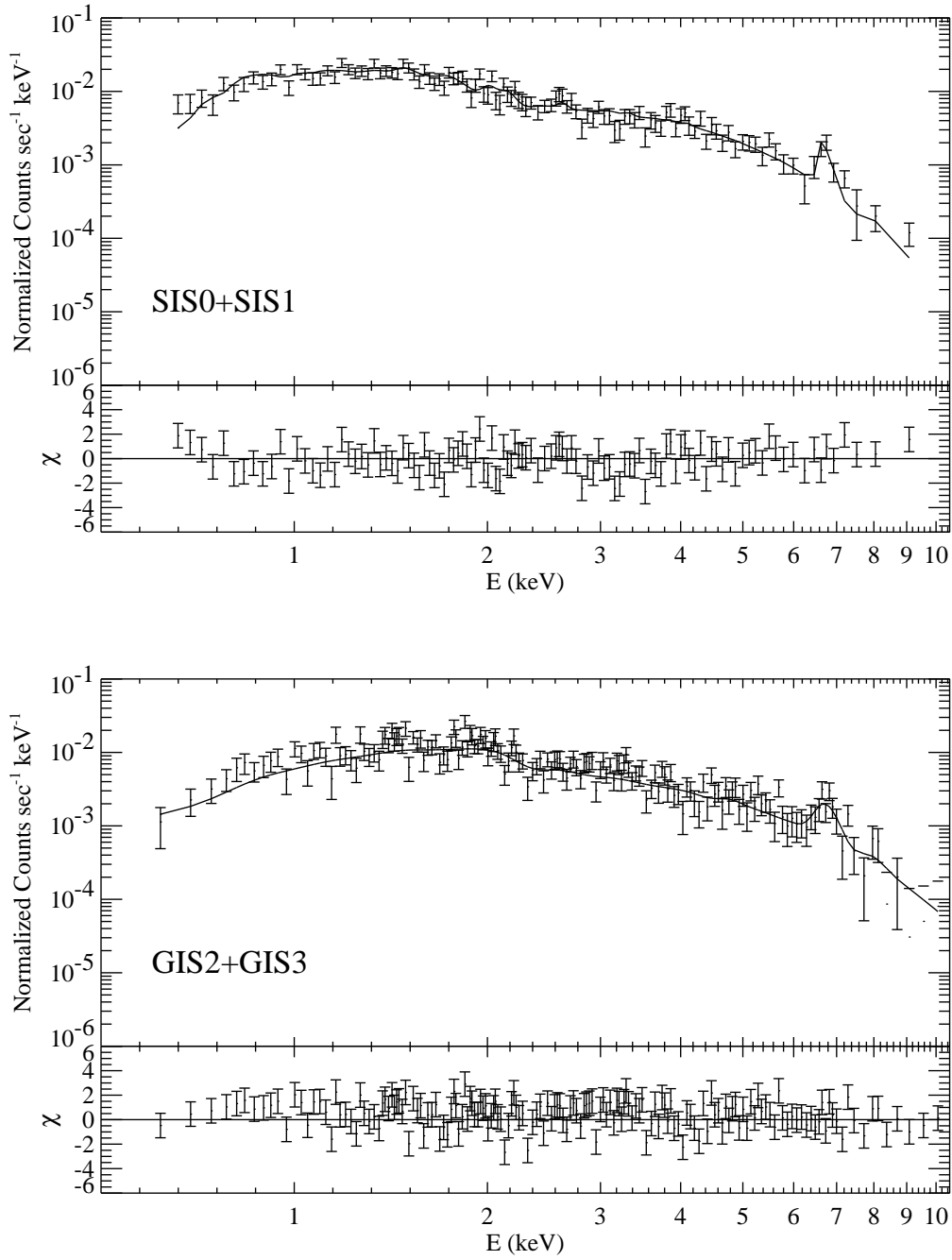


Fig. 5.— Sum of a) *SIS0* and *SIS1* and b) *GIS2* and *GIS3* spectra from 1994 Jan along with the χ^2 values for model 2a94; the solid line is the model fit, after being folded through the instrumental response.

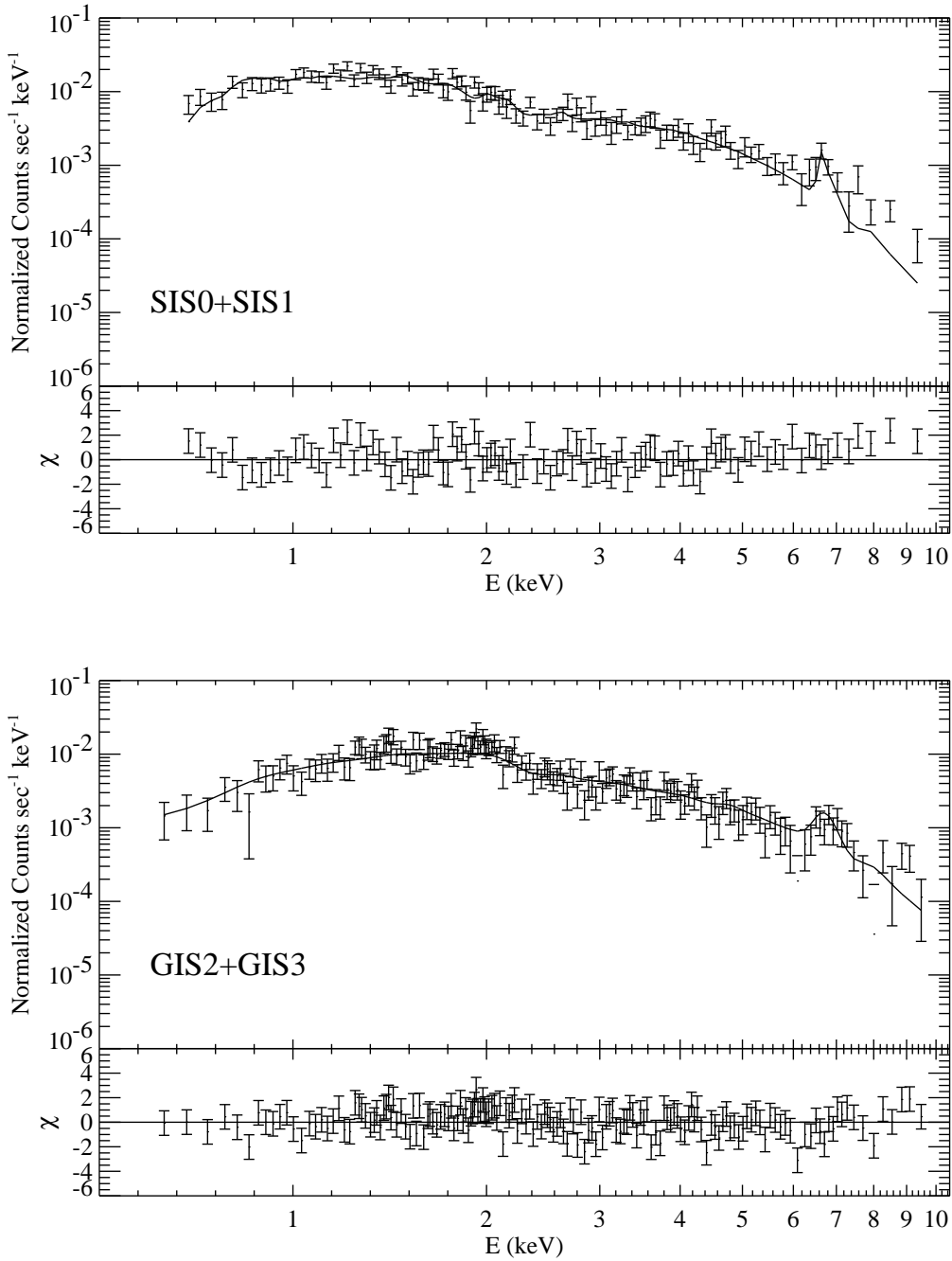


Fig. 6.— Sum of the a) *SIS0* and *SIS1* and b) *GIS2* and *GIS3* spectra from 1996 Jan along with the χ^2 values for the model 2a96; the solid line is the model fit, after being folded through the instrumental response.

from the host galaxy may dominate (Bregman & Pildis 1994).

For each epoch, we simultaneously fit the observed spectra from all four instruments with one and two component thermal emission models using the MEKAL model in XSPEC. The important model parameters are the plasma temperature (kT) and metal abundance (Z), the absorbing column density (N_H) and the normalization $K = (10^{-14}/4\pi D^2) \int n_e^2 dV$ where D is the distance to the source (cm) and n_e is the electron density (cm^{-3}). For consistency with the χ^2 minimization procedure, all spectra were binned to contain at least 20 counts per bin. The best fit parameters and 90% confidence limits for selected parameters are given in Table 3.

Models 1t94 and 1t96 are single temperature fits to the 1994 Jan and 1996 Jan observations respectively. These fits are about the same within the errors, indicating that the supernova spectrum did not change drastically over this two year period. Closer inspection shows that the single temperature fits 1t94 and 1t96 yield significantly higher temperatures $kT \gtrsim 6.5 \text{ keV}$ than either the $kT = 1.0 - 3.9 \text{ keV}$ deduced from earlier *ROSAT* observations of SN1986J Bregman & Pildis (1992) or the $kT \sim 3.0 \text{ keV}$ deduced for SN1978K Petre *et al.* (1994). Also, the 90% confidence limits on the absorbing column density ($\log N_H = 21.18 - 21.42$) are significantly lower than the *PSPC* limits on the absorbing column and the absorbing column deduced from other observations.

From 21 cm observations, Heiles (1975), finds that the H I column density within our galaxy along this line of sight is $N(\text{H I}) = 7.3 \times 10^{20} \text{ cm}^{-2}$. Rupen *et al.* (1987) used VLA observations at 21 cm to measure a column density of $N(\text{H I}) = 2 \times 10^{21} \text{ cm}^{-2}$ within NGC 891 along our line of sight toward SN1986J. Therefore, the total H I column along the line of sight to the supernova is $N(\text{H I}) = 2.7 \times 10^{21} \text{ cm}^{-2}$, corresponding to an optical extinction $A_V = 1.5$, consistent with that used by Leibundgut *et al.* (1991). The X-ray absorbing column includes both the neutral and the warm ionized components along the line of sight. By comparing the mean vertical distributions of H I and H II at the solar circle (Dickey & Lockman 1991; Reynolds 1991), we estimate that the H I column density is about 75% of the total H I + H II column. Therefore, the total X-ray absorbing column density should be about $\log N_H = 21.56$, about 40% larger than the 90% confidence upper limit from our single temperature model fits.

The lack of agreement between the *ASCA* absorbing column and the other observations is unsurprising; because of the lack of sensitivity $\lesssim 0.8 \text{ keV}$, we do not expect the *ASCA* observations to strongly constrain the absorbing column. Furthermore, because the *ASCA* spectra contain X-ray emission from at least three components (SN1986J, diffuse emission from NGC 891, and the nearby point source in the disk), a single temperature spectrum model is an obvious oversimplification. In the following, we examine a range of two-temperature models in which the absorbing column associated with the stronger (high temperature) component is constrained to the range $N_H = (2.75 - 7.25) \times 10^{21} \text{ cm}^{-2}$, consistent with our *ROSAT PSPC* spectra. Models 2a94, 2b94 and 2c94 are two-temperature fits to the 1994 Jan *ASCA* spectra in which the absorbing column associated with the high temperature component was fixed at three different values within

Table 3. ASCA Spectrum Models

Model	χ^2/N	High Temperature Component ^a				Model Flux ^b	
		kT_1 (keV)	Z_1^c	$N_{H,1}^d$	K_1^e	$F_{0.5-2.5}$	F_{2-10}
2a94	360.9/334	6.63(5.99-7.39)	1.06(0.78-1.38)	0.5	1.31(-3)	0.606	1.63
2ac94	395.4/334	5.66(5.18-6.21)	0.98(0.74-1.26)	0.5	1.39(-3)	0.597	1.57
2af94	361.0/334	6.62(5.98-7.37)	1.0	0.5	1.32(-3)	0.606	1.61
2b94	394.0/334	10.3	1.63	0.275	1.07(-3)	0.633	1.70
2c94	380.6/334	4.82	0.99	0.725	1.52(-3)	0.590	1.54
1t94	372.4/334	9.24(8.16-11.3)	1.36(0.98-1.96)	0.20(0.15-0.23)	1.11(-3)	0.611	1.67
2a96	328.0/314	5.37(4.86-5.99)	0.64(0.42-0.90)	0.5	1.18(-3)	0.528	1.17
2ac96	348.9/314	4.50(4.14-4.92)	0.66(0.45-0.89)	0.5	1.27(-3)	0.520	1.12
2af96	333.2/314	5.36(4.88-5.95)	1.0	0.5	1.09(-3)	0.524	1.20
2b96	354.5/314	8.55	0.81	0.275	9.69(-4)	0.547	1.25
2c96	344.3/314	3.99	0.72	0.725	1.37(-3)	0.515	1.11
1t96	326.2/314	7.84(6.72-9.51)	0.72(0.43-1.07)	0.16(0.12-0.20)	0.99(-3)	0.532	1.21

^aFor the two temperature models, the low temperature component was fixed with $K_2 = 5.3 \times 10^{-5}$, $Z_2 = 1$, $\log N_H = 21.0$. Models 2a9X, 2af9X, 2b9X and 2c9X had $kT_2 = 0.62$ keV, while models 2ac9X had $kT_2 = 0.26$ keV.

^bdetected flux in units 10^{-12} erg s⁻¹ cm⁻²

^cFe abundance relative to solar

^dabsorbing column in units 10^{22} cm⁻²

^espectrum normalization coefficient $K_i \equiv (10^{-14}/4\pi D^2) \int n_e^2 dV$ where D is the distance to the source (cm) and n_e is the electron density (cm⁻³)

the range allowed by the Jan 1993 *ROSAT PSPC* observation. Models 2a96, 2b96 and 2c96 are the corresponding sequence of two-temperature fits to the 1996 Jan *ASCA* spectra. In all of the two-temperature fits, the parameters associated with the low temperature component were fixed; in models 2a9X, 2b9X and 2c9X, the temperature and normalization values were chosen by fitting models to the individual *SIS* instruments at both epochs. The absorbing column for the low temperature component was fixed at $\log N_H = 21.0$, consistent with Galactic absorption along the line of sight to NGC891. Model 2ac9X is the same as model 2a9X except $kT_2 = 0.26$ keV, consistent with the *PSPC* observations of the diffuse emission around NGC891 (Bregman & Pildis 1994; Bregman & Houck 1996). Model 2af9X is the same as model 2a9X except that the metallicity is fixed at solar.

Models 2a94 and 2a96 (and 2ac9X) are perhaps the most likely in that the absorbing column associated with the high temperature component (presumably due to the supernova) is close to the *ROSAT PSPC* best fit value, $\log N_H = 21.7$. Although the 90% confidence limits overlap, these models indicate that the high temperature component cooled slightly from $kT = 5.1 - 7.4$ keV in 1994 Jan to $kT = 4.1 - 6.0$ keV in 1996 Jan. In models 2af9X, with the metallicity fixed at solar, the temperature decrease is slightly more significant since the 90% confidence limits no longer overlap. There is also some indication that the metal abundance may have changed from $0.74 - 1.4$ solar in 1994 Jan to $0.42 - 0.90$ solar in 1996 Jan. Models 2b9X and 2c9X help determine the sensitivity of the two-temperature fits to errors in the absorbing column associated with the high temperature component. Varying the absorbing column between $N_H = (2.75 - 7.25) \times 10^{21}$ cm⁻², caused the best fit temperature of the hotter component to vary between $kT = 4.8 - 10.3$ keV in 1994 Jan, and between $kT = 3.99 - 8.55$ keV in 1996 Jan. Underestimating the absorbing column leads to large increases in the best fit temperature, but overestimating the absorbing column leads to only a relatively small decrease in the fit temperature. Comparison of models 2a9X and 2ac9X shows that a factor of 2.4 decrease in the temperature of the cool component decreases the best fit temperature of the hot component by only about 15%.

The measured X-ray fluxes are relatively insensitive to these uncertainties in the best fit spectrum. Averaging all the model fits at the two epochs, we find that the 0.5-2.5 keV flux changed from about 6.07×10^{-13} erg s⁻¹ cm⁻² in 1994 Jan to about 5.28×10^{-13} erg s⁻¹ cm⁻² in 1996 Jan, corresponding to a decrease of 13.0%. The 2-10 keV flux changed from about 1.62×10^{-12} erg s⁻¹ cm⁻² in 1994 Jan to about 1.17×10^{-13} erg s⁻¹ cm⁻² in 1996 Jan, corresponding to a decrease of 27.8%. If our measured 2-10 keV fluxes are due entirely to the supernova, we estimate that the unabsorbed supernova luminosity was of $L_X(2 - 10 \text{ keV}) = 2.04 \times 10^{40}$ erg s⁻¹ in 1994 Jan and $L_X(2 - 10 \text{ keV}) = 1.47 \times 10^{40}$ erg s⁻¹ in 1996 Jan, for 10 Mpc distance and $\log N_H = 21.7$.

We expect that the 0.5-2.5 keV band contains a strong constant background due to diffuse emission in the galaxy, but that the supernova should dominate in the 2-10 keV band, although there may be some additional background due to unresolved point sources in the disk. If the supernova continued to dim $\propto t^{-2}$ between 1994 Jan (age 11.06 yrs) and 1996 Jan (age 13.09 yrs),

we would expect the flux to decrease by $1 - (11.06/13.09)^2 = 28.6\%$, consistent with the observed decrease in 2.0-10 keV flux. In the 0.5-2.5 keV band, we can write the ratio (r) of the 1996 Jan flux to the 1994 Jan flux as

$$r = \frac{s_{96} + g}{s_{94} + g} \quad (1)$$

where s_{94} and s_{96} are the fluxes from the supernova at the two epochs and g is the flux contribution from diffuse emission in NGC 891. If the supernova is dimming $\propto t^{-2}$, then $s_{96}/s_{94} = 0.714$. The 1994 Jan ratio of the galaxy flux to the supernova flux can be written

$$\frac{g}{s_{94}} = \left(\frac{1}{f} - 1\right) \left(\frac{11.06}{t}\right)^2 \quad (2)$$

where $f \equiv s_t/(s_t + g)$ is the supernova fraction of the total 0.5-2.5 keV emission within a $3'$ radius of the supernova at age t years. Using our *ROSAT* data to measure f and assuming that the supernova is dimming $\propto t^{-2}$ and all other X-ray sources are constant, we expect the 0.5-2.5 keV flux to decrease by about 10%, consistent with the observed decrease of 13.0% within the errors. Therefore, the *ASCA* flux measurements are consistent with SN1986J continuing to dim $\propto t^{-2}$ over the energy range 0.5-10 keV between 1994 Jan and 1996 Jan.

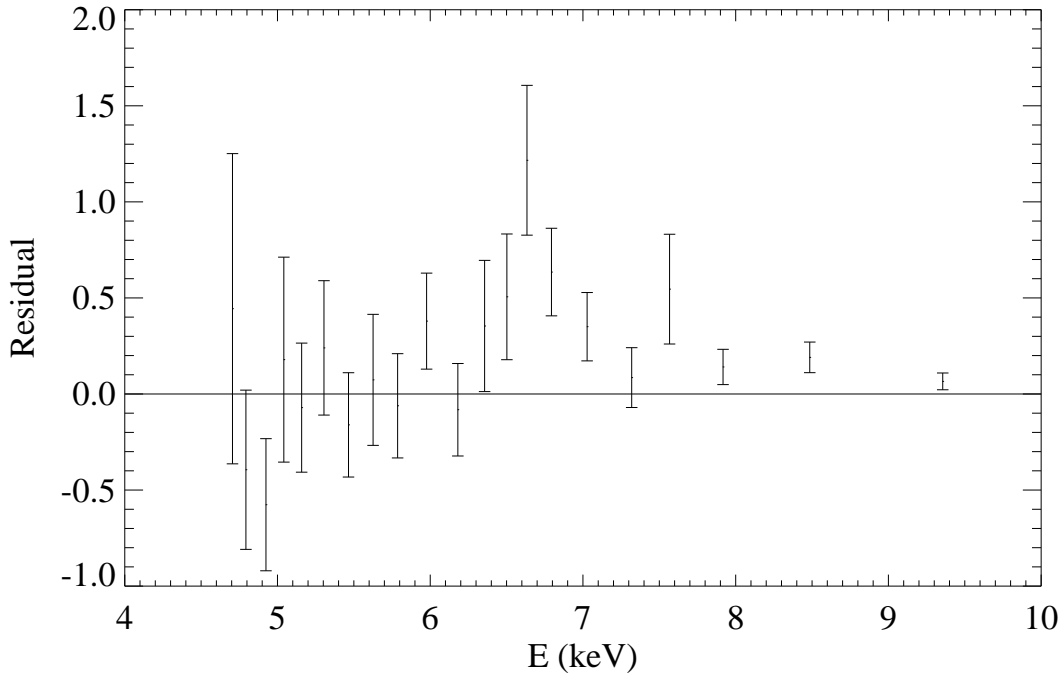


Fig. 7.— Iron line at 6.7 keV shown as residuals after fitting a 5.37 keV Bremsstrahlung continuum to the sum of the *SIS0* and *SIS1* spectra from 1996 Jan. The residuals are plotted in units of 10^{-3} normalized counts $\text{sec}^{-1} \text{keV}^{-1}$.

Because it represents the clearest means of discriminating between the two proposed models for the X-ray emission, the width of the Fe K line at 6.7 keV is an important observable

parameter. By fitting a Gaussian profile to the observed line, we set a 90% confidence upper limit of $\sigma = 0.17 \text{ keV}$ on the line width, for a line centered at 6.79 keV ; the best fit line width is $\sigma = 0.10 \text{ keV}$ (Fig. 7). Unfortunately, this upper limit is not strong enough to discriminate between the model predictions.

3. Discussion

Based on a crude model for the radio light curves of SN 1986J, Chevalier (1987) estimated a value of $\dot{M}_{-4}/v_{w1} \sim 1$, where \dot{M}_{-4} is the progenitor mass loss rate in units of $10^{-4} M_{\odot} \text{ yr}^{-1}$ and v_{w1} is the wind velocity in units of 10 km s^{-1} , and an explosion date in late 1982. This model led to the prediction of X-ray emission from the reverse shock front with a luminosity $\sim 10^{40} \text{ ergs s}^{-1}$ and a temperature of $(1 - 4) \times 10^7 \text{ K}$. These predictions were roughly verified by Bregman & Pildis (1992). A more detailed model for the radio emission by Weiler, Panagia, & Sramek (1990) led to $\dot{M}_{-4}/v_{w1} = 2.4$ and an explosion time in late 1982. However, this model did involve assumptions about a mixed absorbing/emitting region and the temperature of the surrounding wind is a factor in determining the circumstellar density from the radio light curves (Lundqvist & Fransson 1988), so this value for \dot{M}_{-4}/v_{w1} is uncertain.

CF present details for 2 circumstellar interaction models with $\dot{M}_{-4}/v_{w1} = 0.5$ at an age of 10 years. The red supergiant model has $L = 4 \times 10^{39} \text{ ergs s}^{-1}$, but a temperature of only $3 \times 10^6 \text{ K}$ because of the steep density gradient; the shock wave is radiative. The power law model ($n = 8$) has a lower luminosity by a factor of 2, but the temperature is about 10^7 K ; the shock wave became adiabatic at an age of 0.1 yr. In the first case, the luminosity scales roughly as \dot{M}/v_w and the second as $(\dot{M}/v_w)^2$ provided the adiabatic assumption remains applicable. The observed temperature suggests that something like the power law case (i.e. a relatively flat density profile) is more relevant to SN 1986J, but with a higher value of \dot{M}/v_w . The current X-ray observations point to a value of \dot{M}_{-4}/v_{w1} of a few.

A problem with the reverse shock model was raised by Chugai (1993), who noted that the VLBI observations of Bartel, Rupen, & Shapiro (1989) imply an average velocity of $13,000 \text{ km s}^{-1}$. The problem is that an object with typical supernova parameters expanding into the dense medium discussed above would be decelerated to considerably lower velocities. Although Chugai (1993) considers a particular supernova density profile with $n = 8$, it seems that the argument is widely valid. The 2 models of CF discussed above have peak ejecta velocities of 4300 km s^{-1} and 5000 km s^{-1} , respectively, at an age of 10 years. With the higher circumstellar density inferred for SN 1986J, the velocities would be even lower. However, the VLBI image produced by Bartel et al. (1991) in late 1988 shows that the source has a complex structure; it is made up of an incomplete shell with several protrusions. The angular diameter across the peak brightness of the shell is about 1.6 milliarcsec. At an age of 6 years, this corresponds to a radial velocity of $6,300 \text{ km s}^{-1}$. The origin of the protrusions is not certain, but the simulations of Blondin, Lundqvist, & Chevalier (1996) show that protrusions can develop if there is an angular density gradient in some

direction. Protrusions would develop most naturally along one axis, which is not the case for SN 1986J, but the simulations do show the possibility of forming the required protrusions.

To be more specific, we consider the power law density profile models discussed in section 2 of CF. We take $\dot{M}_{-4}/v_{w1} = 2.4$ (Weiler et al. 1990 and the above discussion of X-ray luminosity) and $n = 7$ in order to maximize the reverse shock gas temperature. The reference density, ρ_r , is defined to be the density at a velocity of $5,000 \text{ km s}^{-1}$ and age of 1 year, and can be $2 \times 10^{-16} \text{ gm cm}^{-3}$ for a low mass explosion. Then, at $t = 6 \text{ yr}$, the outer shock velocity is $6,000 \text{ km s}^{-1}$, which corresponds to an average shock velocity of $7,400 \text{ km s}^{-1}$. The average velocity in the shell would be somewhat lower than this and in accord with the VLBI shell velocity. At $t = 10 \text{ yr}$ (late 1992), the outer shock velocity is $5,400 \text{ km s}^{-1}$, which leads to a post-reverse shock temperature of $1.4 \times 10^7 \text{ K}$. This temperature is somewhat lower than the observed one, but the outer shock should have a temperature of $4 \times 10^8 \text{ K}$. This component should have a lower luminosity than the cool component, although nonequilibrium effects could give rise to enhanced line emission. It is also possible that the supernova density profile is complex and the shock front is in a particularly flat section.

In this model, the reverse shock makes a transition from radiative to non-radiative at an age of about 2 years. At the time of the observations, the X-ray luminosity should tend to decrease as t^{-1} . The observed decline is steeper than this (t^{-2}). The steeper decline can be produced if the circumstellar density drops more rapidly than r^{-2} (Fransson, Lundqvist, & Chevalier 1996). The very high circumstellar density deduced for SN 1986J suggests that it may be associated with a short-lived mass loss event prior to the supernova explosion. The circumstellar column density outside the outer shock front is $2.4 \times 10^{21} \text{ cm}^{-2}$ at an age of 10 yr. Because of the transition to an adiabatic shock wave and the low value of n , the column density of cool gas behind the reverse shock front is probably less than this. The ability of this gas to absorb is further reduced by hydrodynamic instabilities. When the above value is compared to the observed values of N_H , it is plausible that the circumstellar medium is a significant contributor to the total column density to the the supernova. In this model, the circumstellar N_H declines as $t^{-0.8}$.

The reverse shock model is thus able to account for the general features of the observed X-ray emission, although it fails to reproduce some specific features. We have not pursued extensions of the model, such as the possibility of a density gradient dropping more rapidly than r^{-2} , because of the limited data that are available. In the alternative model of Chugai (1993), the X-ray emission is from shocked clouds. There is possible evidence for a clumpy circumstellar medium in that SN 1986J shows narrow hydrogen emission; the FWHM of the $H\alpha$ line corresponds to an expansion velocity of 530 km s^{-1} (Rupen et al. 1987; Leibundgut et al 1991). However, the observed X-ray temperature requires a shock velocity of about $2,000 \text{ km s}^{-1}$, so that the same clouds cannot be responsible for the optical and X-ray emission. The cloud model has many free parameters (the cloud filling factor, density contrast, size, and the variation of these with radius), so it is likely that a model fit can be obtained; it is the uniqueness of the model that is in question. There is the possibility of observationally distinguishing the models because the cloud model involves

expansion velocities about a factor 3 smaller than those in the reverse shock model. In both cases, the emission from the receding gas is absorbed by the supernova, so that the observed emission is primarily blueshifted. Our measurement of the Gaussian line width σ corresponds to a 90% confidence upper limit of 20000 km s^{-1} FWHM. Unfortunately, this limit is too weak to distinguish between the two models, but future X-ray missions, such as *AXAF*, may be able to provide an answer.

Although our X-ray light curve so far has only a few points, the light curve is the least ambiguous piece of evidence because the high resolution observations give us a high degree of confidence that the light curve is not seriously contaminated by emission from nearby X-ray sources. In contrast, the interpretation of the *ASCA* spectra is somewhat unclear because of the significant level of contamination from other sources of X-ray emission in the field of view, and in particular from point sources in the disk and diffuse emission from the halo of NGC891. Despite the lack of information on the spectral characteristics of the contaminating sources, we can estimate the relative contributions from each source. The diffuse emission from the X-ray halo is quite soft, with $kT \lesssim 1 \text{ keV}$, and contributes around 40% of the flux below about 1 keV. While the spectra of the point sources in the disk are unknown, the change in 2-10 keV flux observed from 1994 Jan to 1996 Jan is consistent with the supernova dominating the emission in this band.

X-ray bright supernovae like SN1986J appear to be relatively rare (Houck & Bregman 1996). Therefore, this object represents an excellent opportunity to study the physics of an extreme example of the interaction of a supernova with a dense circumstellar environment and we hope to continue monitoring X-ray emission from SN1986J as long as possible. Despite the relatively rapid decline in X-ray luminosity, future high spatial resolution observations with *ROSAT* and *AXAF* should allow us to track the light curve and to follow changes in the spectrum for several years to come. Observations with *AXAF* should be particularly useful for providing high quality spectra and, thus, line widths.

4. Acknowledgements

We would like to thank Keith Arnaud, Ken Ebisawa, and the *ASCA-GOF* for their assistance with the *ASCA* data analysis. Financial support for this work was provided by NASA grants NAGW-2135, NAGW-4448, NAG5-2732, and NAG5-3057.

REFERENCES

- Bartel, N. Rupen, M. P., & Shapiro, I. I. 1989, *ApJ*, 337, L85
- Bartel, N. Rupen, M. P., Shapiro, I. I., Preston, R. A., & Ruis, A. 1991, *Nature*, 350, 212
- Blondin, J. M., Lundqvist, & Chevalier, R. A. 1996, *ApJ*, 472, 257

- Bregman, J.N., & Houck, J., 1996, ApJ, in press.
- Bregman, J.N., & Pildis, R.A., 1992, ApJ, 398, L107
- Bregman, J.N., & Pildis, R.A., 1994, ApJ, 420, 570
- Canizares, C., Kriss, G.A., & Feigelson, E.D., 1982, ApJ, 253, L17
- Chevalier, R.A., 1982, ApJ, 258, 790
- Chevalier, R.A., 1987, Nature, 329, 611
- Chevalier, R.A., & Fransson, C., 1994, ApJ, 420, 268 (CF)
- Chugai, N.N., 1993, ApJ, 414, L101
- Dickey, J.M., & Lockman, F.J., 1990, ARA&A, 28, 215
- Fabian, A.C., & Terlevich, R., 1996, MNRAS, 280, L5
- Fransson, C., Lundqvist, & Chevalier, R. A. 1996, ApJ, 461, 993
- Gorenstein, P., Hughes, J.P., & Tucker, W., 1994, ApJ, 420, L25
- Heiles, C., 1975, A&AS, 20, 37
- Houck, J, & Bregman, J., 1996, “X-Ray Imaging and Spectroscopy of Cosmic Hot Plasmas: International Conference on X-Ray Astronomy” (Tokyo), in press
- Leibundgut, B., Kirshner, R.P., Pinto, P.A., Rupen, M.P., Smith, R.C., Gunn, J.E., and Schneider, D.P., 1991, ApJ, 372, 531
- Lundqvist, P., & Fransson, C. 1988, A&A, 192, 221
- Petre, R., Okada, K., Mihara, T., Makishima, K., & Colbert, E.J.M., 1994, PASJ, 46, L115
- Raymond, J.C., Cox, D.P., & Smith, B.W., 1976, ApJ, 204, 290
- Reynolds, R.J., 1991, in The Interstellar Disk-Halo Connection in Galaxies, ed. H. Bloemen (Dordrecht: Kluwer), 67
- Rupen, M.P., Van Gorkom, J.H., Knapp, G.R., Gunn, J.E., & Schneider, D.P., 1987, AJ, 94, 61
- Ryder, S.D., Staveley-Smith, L., Dopita, M.A., Petre, R., Colbert, E., Malin, D.F., & Schlegel, E.M., 1993, ApJ, 416, 167
- Schlegel, E., 1995, Rep. on Prog. in Phys., 58, 1375
- Tanaka, Y., 1989, Physics of Neutron Stars and Black Holes, ed. Y. Tanaka, (Tokyo: Universal Academy Press, Inc.), 431

Tanaka, Y., 1993, IAUC, 5753

Weiler, K. W., Panagia, N., & Sramek, R. A. 1990, ApJ, 364, 611

Zimmerman, H., *et al.* , 1993, IAUC, 5748